Fig. 1. A map of A_0 calculated in the range of phase angles 12–22°.

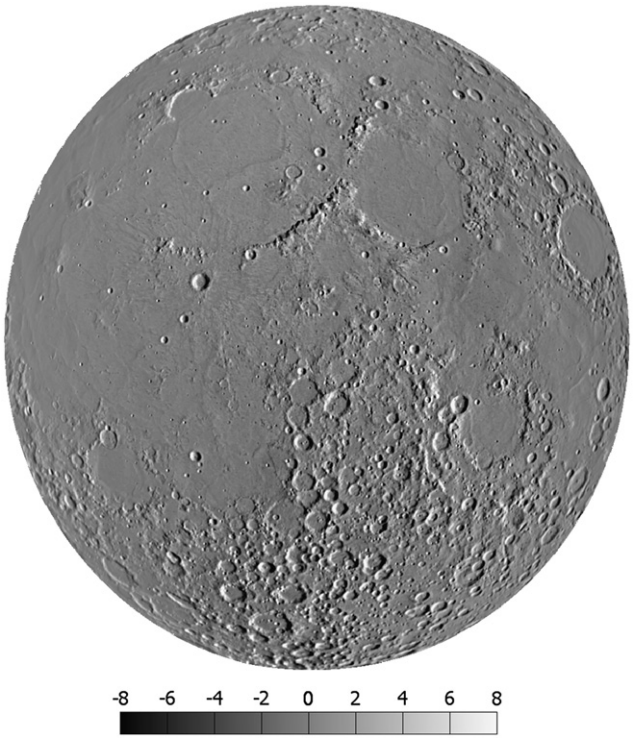

Fig. 2. A map of longitudinal topographic slopes determined on a 3.2 km base; the map is calculated using 12 images in the range of phase angles 12–22°.

a result of albedo extrapolation defined with formula (7) to $\alpha=0$ using 12 images obtained at phase angles 12°–22°. The distribution of A_0 is similar to that of the equigonal albedo $A_{eq}(\alpha)$ at any moderate phase angle and characterizes the reflection properties of the lunar surface materials. It should be emphasized that the albedo map in Fig. 1 does present real brightness distribution at $\alpha=0$, as it ignores variations of opposition-effect amplitudes that are not described by formula (7). The opposition spike has components of shadow-hiding and coherent backscattering effects (e.g., Hapke, 1993; Shkuratov et al., 2004). To include these in the analysis, a more complicated approximation of the phase function is needed (Velikodsky et al., 2010).

Fig. 2 shows a distribution of the longitudinal component r_l of the topographic slope calculated on a 3.2 km base. The distribution in Fig. 3 shows realistic values of slope up to 8°. This is in agreement with our assumption that topographic slopes on bases provided by Earth-based telescope observations are small. Some sites demonstrate slopes reaching 20°. The maximal value of slope we obtained in this analysis is 22°, observed at the selenographic coordinates $l=0.2°$, $b=21.6°$ in Montes Apenninus. This new map of longitudinal slopes coincides well with our previous results (Korokhin and Akimov, 1997).

Shown in Fig. 4 is a map of the parameter μ of function (7) determined in the range of phase angles 12–22°. The distribution describes the steepness of the phase dependence of the lunar surface brightness. The parameter μ can be determined using many calibrated images; whereas, a phase-angle-ratio image includes only two components. In any case, the images of the phase ratio and of the parameter μ calculated for the same phase angle range should be very similar. As one can see, the parameter μ demonstrates an inverse correlation with albedo: the higher the steepness μ, the lower the albedo. This is in agreement with our previous results (Shkuratov et al., 1994; Korokhin and Akimov, 1997; Kreslavsky et al., 2000; Kreslavsky and Shkuratov, 2003; Kaydash et al., 2009b).

The albedo A_0 and steepness μ maps calculated using the described algorithm are almost free from the influence of the lunar topography (see Figs. 1 and 4). Figs. 5 and 6 show the case, if we ignore the compensation for the topography, i.e., when the phase-function parameters (7) A_0 and μ are calculated without accounting for the lunar relief. The difference, especially between the steepness distributions (see Figs. 4 and 6), seems to be dramatic. In the case of Figs. 1 and 4 some traces of relief are observed near the limb and the polar regions. This probably is caused by neglecting the latitudinal component of local slopes and the presence of areas on the source images with too large emergence and incidence angles.

Errors in using the approximation with the function (7) are shown in Fig. 7. Typical values of the error (the standard deviation divided by A_0 in percents) are 0.35–0.5% for maria, 0.4–1.0% for highlands, and up to 4% for bright craters. Areas near the limb have maximal values of errors (up to 20%). Small errors are observed in maria, because their surface is relatively flat. Moreover, the function (7) works for maria better than for highlands and bright craters. Thus, higher errors for highlands and bright craters are caused by more complicated topography in addition to the simplified function with one exponent (7) being not representative of the phase curves of highlands. High errors near the limb appear due to the presence of real shadows in addition to poor image co-registration caused by neglecting real heights of the lunar sites in the compensation for libration. In spite of some shortcomings of the technique, the approximation of phase function without accounting for the influence of the lunar relief gives much larger errors.

4. Comparison with LALT data

As has been noted, recent altimetric data have been obtained with the LALT (laser altimeter) aboard the spacecraft Kaguya (Araki et al., 2009). The LALT was able to obtain a range of data on a global scale along the satellite's trajectory including the high latitude region above 75° that has never been measured by an